

1 **The Brazilian Amaryllidaceae as a source of acetylcholinesterase inhibitory alkaloids**

2
3
4
5
6
7
8
9
10
11
12
13
14
15
16
17
18
19
20
21
22
23
24
25
26
27
28
29
30
31
32
33
34
35
36
37
38
39
40
41
42
43
44
45
46
47
48
49
50
51
52

Jean Paulo de Andrade · Raquel B. Giordani · Laura Torras-Claveria · Natalia Bele'n Pigni · Strahil Berkov · Merce` Font-Bardia · Teresa Calvet · Eduardo Konrath · Kelly Bueno · Liana G. Sachett · Julie H. Dutilh · Warley de Souza Borges · Francesc Viladomat · Amelia T. Henriques · Jerald J. Nair · Jose` Angelo S. Zuanazzi · Jaume Bastida

J. P. de Andrade · L. Torras-Claveria ·
N. B. Pigni · S. Berkov · F. Viladomat ·
J. J. Nair · J. Bastida
Departament de Productes Naturals, Biologia Vegetal i
Edafologia, Facultat de Farma`cia, Universitat de
Barcelona, Av. Diagonal 643, 08028 Barcelona, Spain
e-mail: jaumbastida@ub.edu

J. P. de Andrade · R. B. Giordani · E. Konrath ·
K. Bueno · L. G. Sachett · A. T. Henriques ·
J. A. S. Zuanazzi
Faculdade de Farma`cia, Universidade Federal do Rio
Grande do Sul, 2752 Ipiranga Av.,
Porto Alegre 90610-000, Brazil

J. P. de Andrade · W. de Souza Borges
Departamento de Qui`mica, Universidade do Espi`rito
Santo, Vitoria, ES 29075-910, Brazil

S. Berkov
AgroBioInstitute, 8 Dragan Tzankov blvd., 1164 Sofia,
Bulgaria

M. Font-Bardia
Centres Cientifics i Tecnològics, Universitat de
Barcelona, Sole` i Sabaris 1-3, 08028 Barcelona, Spain

T. Calvet
Cristal·lografia, Mineralogia i Dipos·sits Minerals, Facultat
de Geologia, Universitat de Barcelona, Marti` i Franque`s s/
n, 08028 Barcelona, Spain

J. H. Dutilh
Departamento de Bota`nica, Universidade de Campinas,
Cidade Universita`ria, Campinas 13083-970, Brazil

53 **ABSTRACT:**

54

55 Nine Brazilian Amaryllidaceae species were studied for their alkaloid composition and
56 acetylcholinesterase (AChE) inhibitory activity via GC–MS and a modified Ellman assay, respectively.

57 A total of thirty-six alkaloids were identified in these plants, of which *Hippeastrum papilio* and *H.*

58 *glaucescens* exhibited the highest galanthamine content and the best IC₅₀ values against AChE.

59 Furthermore, *Hippeastrum vittatum* and *Rhodophiala bifida* also showed notable AChE inhibitory

60 effects. X-ray crystallographic data for four galanthamine-type compounds revealed significant

61 differences in the orientation of the N-methyl group, which are shown to be related to AChE inhibition.

62

63

64

65 **INTRODUCITON**

66

67 The Amaryllidaceae alkaloids represent a large group of isoquinoline alkaloids derived from the
68 common biogenetic precursor O-methylnorbelladine through oxidative phenolic coupling, leading to
69 eight distinct structural-types (Bastida et al. 2006). The galanthamine- type skeleton has been the focus
70 of numerous studies since the AChE inhibitor galanthamine was approved by the FDA for the clinical
71 management of mild to moderate Alzheimer’s disease (AD) (Maelicke et al. 2001). Although the
72 chemical synthesis of galanthamine has been achieved on several occasions, natural sources still
73 constitute the bulk of its commercial supply chain (Berkov et al. 2011). Apart from this, the other
74 structural representatives of the Amaryllidaceae are known for a diverse array of biological activities
75 including, antitumoral, antiviral, antiparasitic, anti-inflammatory, psychopharmacological and
76 interactions with human cytochrome P450 3A4 (Vrijsen et al. 1986; C, itog̃lu et al. 1998; da Silva et al.
77 2006; McNulty et al. 2007, 2009; Zupko’ et al. 2009; Giordani et al. 2010). These attributes have
78 showcased the Amaryllidaceae as a promising resource for new and bioactive molecules.

79 The high resolution power of the capillary column technique in gas chromatography (GC) together with
80 the ready availability of libraries of electron impact mass spectrometry (EI–MS) data in the literature
81 facilitate the rapid identification and quantification of known alkaloids. This has been shown to be
82 particularly useful to studies of the Amaryllidaceae, extracts of which contain a large number of
83 alkaloids (Kreh et al. 1995; Wagner et al. 2003). To this extent, several southern Brazilian
84 Amaryllidaceae species have been examined for their alkaloid content and biological activity (da Silva
85 et al. 2006, 2008; Pagliosa et al. 2010; Giordani et al. 2011a, b; de Andrade et al. 2011). In the present
86 study, a GC–MS analysis was undertaken on nine Amaryllidaceae species which allowed for the
87 identification of thirty-six alkaloids belonging to seven skeleton-types. Furthermore, an AChE inhibitory
88 activity assay was carried out with both isolated compounds and alkaloid-rich fractions. In addition, X-
89 ray crystallographic analysis was carried out on some galanthamine derivatives, providing insights to the
90 structural features attending AChE activity.

91

92 MATERIALS AND METHODS

93

94 Chemicals

95 Galanthamine (27) and 11b-hydroxygalanthamine (32) used for X-ray crystallography were previously
96 obtained from *Hippeastrum papilio* (de Andrade et al. 2011). Sanguinine (28) and narwedine (31) were
97 obtained in previous works from *Crinum kirkii* Chemicals Galanthamine (27) and 11b-
98 hydroxygalanthamine (32) used for X-ray crystallography were previously obtained from *Hippeastrum*
99 *papilio* (de Andrade et al. 2011). Sanguinine (28) and narwedine (31) were obtained in previous works
100 from *Crinum kirkii* (Machocho et al. 2004) and *Leucojum aestivum* (Berkov et al. 2008a), respectively.
101 MeOH (HPLC grade), CHCl₃, Me₂CO, H₂SO₄ and NH₄⁺ (analytical grade) were purchased from SDS
102 (France). Acetylthiocholine iodide (ATCI), acetylcholinesterase (AChE) from electric eels (type VI-S
103 lyophilized powder), and 5,5 V-dithiobis[2-nitrobenzoic acid] (DTNB) were obtained from Sigma-
104 Aldrich Chemie (Steinheim, Germany). The n-hydrocarbon mixture (C₉–C₃₆, Restek, Cat no. 31614)
105 was supplied by Teknokroma (Spain). Galanthamine (purity 99 %) used for the calibration curves was
106 previously obtained by the authors, and codeine (purity 99 %) used as internal standard was purchased
107 from Sigma Aldrich (St. Louis, MO, USA).

108

109 Plant material

110 The species *H. papilio* (Ravenna) Van Scheepen (bulbs and leaves, UFRGS–ICN 149428), *Hippeastrum*
111 *vitattum* (L'Her.) Herb. (bulbs, UFRGS–ICN 8889), *Hippeastrum striatum* (Lam.) Moore (bulbs,
112 UFRGS–ICN 9549), *Hippeastrum morelianum* Lem. (bulbs, UNICAMP–UCE 14351), *Hippeastrum*
113 *santacarina* (Traub) Dutilh (bulbs, UFRGS–ICN 149429), *Hippeastrum breviflorum* Herb. (bulbs,
114 UFRGS–ICN 9190), *Hippeastrum glaucescens* (Mart.) Herbert (bulbs and leaves, UFRGS–ICN 8894),
115 *Hippeastrum psittacinum* Herb. (bulbs and leaves, UNICAMP–UCE 143513) and *Rhodophiala bifida*
116 (Herb.) Traub (bulbs, UNICAMP–UCE 136352) were collected and the extracts obtained according to
117 previously described methods (Castilhos et al. 2007; da Silva 2005; da Silva et al. 2008; Pagliosa et al.
118 2010; Giordani et al. 2011a, b; de Andrade et al. 2011; Sebben 2005).

119

120 Sample preparation

121 The plant material (1 g) was crushed and extracted by stirring at rt with MeOH (3.950 ml), the
122 combined macerate filtered and evaporated to dryness under reduced pressure. The crude extract was
123 acidified to pH 2 with 2 % H₂SO₄, neutral material removed using Et₂O (3.925 ml). The aqueous
124 phase was then basified up to pH 11 with NH₃ (25 %, v/v) and extracted with CHCl₃ (3.925 ml) to
125 afford the chloroform extract.

126

127

128

129 GC–MS and identification of alkaloids

130 The chloroform extract (300 μ l) was filtered and then used for subsequent GC–MS analysis. EI–MS
131 spectra were obtained on an Agilent 6890 N GC 5975 inert MSD operating in EI mode at 70 eV (Agilent
132 Technologies, Santa Clara, California, USA) utilizing a DB-5 MS column (30 m \times 0.25 mm \times 0.25 μ m,
133 Agilent Technologies) with an injector temperature of 280 $^{\circ}$ C. The temperature program was as
134 follows: 100–180 $^{\circ}$ C at 15 $^{\circ}$ Cmin⁻¹, 1 min hold at 180 $^{\circ}$ C and 180–300 $^{\circ}$ C at 5 $^{\circ}$ Cmin⁻¹ and 10 min
135 hold at 300 $^{\circ}$ C. The flow rate of carrier gas (Helium) was 0.8 ml min⁻¹ and a split ratio of 1:20 was
136 followed. The alkaloids were identified by comparing their GC–MS spectra and Kovats retention indices
137 (RI) with our in-house library database. This library has been continually updated and reviewed with
138 alkaloids isolated by our group and identified using other spectroscopic techniques such as NMR, UV,
139 CD and MS. Mass spectra were deconvoluted using AMDIS 2.64 software (NIST). Kovats retention
140 indexes (RI) of the compounds were recorded with standard calibration of an n-hydrocarbon mixture
141 (C9–C36).

142 The proportion of each individual component in the alkaloid fractions analysed by GC–MS (Table 1) is
143 expressed as a percentage of the total alkaloids (TIC—total ion current). The area of the GC–MS peak
144 depends not only on the concentration of the corresponding compound but also on the intensity of its
145 mass spectral fragmentation. Although data given in Table 1 do not express a real quantification, they
146 can nevertheless be used for a relative comparison of the alkaloids.

147 Quantification of galanthamine in *H. papilio* The quantification was performed in triplicate using 50 mg
148 of dried material (leaves and bulbs, separately) and codeine as i.s. (50 μ g) in screw-top 2.0 ml Eppendorf
149 tubes. The maceration procedure was carried out with 1 ml of MeOH adjusted to pH 8 with NH₃ (25 %, v/v).
150 After 2 h of extraction at room temperature assisted by 15 min ultrasonic baths every 30 min, the
151 samples were centrifuged at 10,000 rpm for 2 min. An aliquot of 500 μ l of methanolic macerate was
152 acidified with 500 μ l of H₂SO₄ (2 %, v/v) and neutral material removed with chloroform (2 \times 500 μ l).
153 The aqueous fraction was then basified with 200 μ l of NH₃ (25 %, v/v) and alkaloids extracted with
154 CHCl₃ (3 \times 500 μ l). Finally, the purified alkaloid extract was dried under N₂ and redissolved in 100 μ l of
155 CHCl₃ for GC–MS analysis. The GC–MS conditions were the same used for the alkaloid-rich extract
156 (Section GC–MS and identification of alkaloids).

157 Recovering and repeatability of the extraction The extraction recovery was performed as described
158 above by adding 50, 300 and 500 μ g of galanthamine to the dry plant sample (50 mg of powdered bulbs
159 and leaves of *H. papilio*) before the extraction and purification. Intraday (n = 4) and interday (n = 8)
160 repeatability was calculated with 50 mg of dried powdered bulbs of *H. papilio*, extracted, purified and
161 analysed via GC–MS on two different days according to Berkov et al. (2008b).

162

163 Samples for X-ray

164 Narwedine (31) and 11b-hydroxygalanthamine (32) were dissolved in CHCl₃ under a pentane
165 atmosphere and left in the freezer (less than 5 $^{\circ}$ C) for a week. Sanguinine (28) was dissolved in a

166 MeOH:EtOH mixture (1:1, v/v) under a pentane atmosphere and left in the freezer (less than 5 °C) for
167 two weeks. Galanthamine (27) was dissolved in Me₂CO and left in the freezer for a week. Suitable
168 crystals for X-ray analysis were preselected under a light microscope. The crystallographic data of 27
169 and 31 were in agreement with those previously reported (Carrol et al. 1990; Hemetsberger et al. 2004).

171 X-Ray analysis for sanguinine (28)

172 A translucent prism-like specimen of sanguinine with the dimensions 0.192 mm × 0.278 mm × 0.457
173 mm was used for X-ray crystallographic analysis. First, the X-ray intensity data were determined, with a
174 total of 171 frames collected at an exposure time of 1.71 h. The frames were integrated with the Bruker
175 SAINT software package using a narrow-frame algorithm. The integration of the data using a
176 monoclinic unit cell yielded a total of 19,735 reflections to a maximum θ angle of 30.67° (0.70 Å⁻¹
177 resolution), of which 7366 were independent (average redundancy 2.679, completeness = 94.1 %, R_{int} =
178 4.80 %, R_{sig} = 5.54 %) and 6597 (89.56 %) were greater than $2\sigma(F_2)$. The final cell constants of a =
179 9.227(6) Å, b = 15.095(8) Å, c = 9.750(5) Å, β = 102.28(3)°, volume = 1327.2 Å³
180 3, are based upon the refinement of the XYZ-centroids of 142 reflections above $2\sigma(I)$ with
181 $4.944^\circ \times 49.15^\circ$. Data were corrected for absorption effects using the multi-scan method (SADABS).
182 The ratio of minimum to maximum apparent transmission was 0.757.

183 The structure was solved and refined using the Bruker SHELXTL Software Package, with $Z = 2$ for the
184 formula unit, C₁₆H₁₉NO₃. The final anisotropic full-matrix least-squares refinement on F_2 with 375
185 variables converged at $R_1 = 4.08$ %, for the observed data and $wR_2 = 10.17$ % for all data. The
186 goodness-of-fit was 1.047. The largest peak in the final difference electron density synthesis was 0.382
187 e-/Å³ and the largest hole was -0.274 e-/Å³ with an RMS deviation of 0.058 e-/Å³. On the basis of
188 the final model, the calculated density was 1.367 g/cm³ and $F(000)$, 584 e-.

190 X-Ray analysis for 11b-hydroxygalanthamine (32)

191 A prismatic crystal (0.1 × 0.09 × 0.08 mm) was selected and mounted on a MAR345 diffractometer with
192 an image plate detector. Unit-cell parameters were determined from 107 reflections ($3^\circ \times 318^\circ$) and
193 refined by the least-squares method. Intensities were collected with graphite monochromatized Mo K α
194 radiation. 8529 reflections were measured in the range $2.44^\circ \leq \theta \leq 24.10^\circ$, 2419 of which were non-
195 equivalent by symmetry ($R_{int}(on I) = 0.045$). 2135 reflections were assumed as observed applying the
196 condition $I \geq 2\sigma(I)$. Lorentz-polarization was considered, but no absorption corrections were made. The
197 structure was solved by direct methods, using the SHELXS computer program (Sheldrick 2008) and
198 refined by the full-matrix least-squares method with the SHELX97 computer program (Sheldrick 2008),
199 using 8529 reflections, (very negative intensities were not assumed). The function minimized was $R_w =$
200 $\frac{\sum w(|F_o| - |F_c|)^2}{\sum w|F_o|^2}$, where $w = \frac{1}{[\sigma^2(I) + (0.0683P)^2]}$ -1, and $P = \frac{(|F_o|^2 + 2|F_c|^2)}{3}$, f , f' and f'' were taken
201 from International Tables of X-Ray Crystallography (1974). All H atoms were computed and refined,
202 using a riding model, with an isotropic temperature factor equal to 1.2 times the equivalent temperature

203 factor of the atom which are linked. The final R(on F) factor was 0.047, wR(on |F|²) = 0.117 and
204 goodness of fit = 1.069 for all observed reflections. The number of refined parameters was 200. Max.
205 shift/esd = 0.00, mean shift/esd = 0.00. Max. and min. peaks in final difference synthesis were 0.395 and
206 -0.169 e.Å⁻³, respectively.

207

208 AChE inhibitory activity

209 The assay for measuring AChE inhibitory activity was performed as described by Lo'pez et al. (2002).
210 Galanthamine hydrobromide was used as a positive control. A solution of the initial alkaloid-rich extract
211 (chloroform fraction) at 1 mg/ml was taken up in MeOH and diluted further with phosphate buffer to
212 give 100, 10, 1, 0.1, 0.01, 0.001 lg/ml solutions. Only IC₅₀ values less than 100 lg/ml were considered.
213 Compounds 27, 28, 31, and 32 were used in dilutions at the range of 10⁻⁸ to 10⁻³ M. Dilutions at 10⁻⁴
214 M were prepared in MeOH and further dilutions were carried out using phosphate buffer. IC₅₀ of all
215 extracts/compounds were measured in triplicate and the results are presented as a mean ± standard
216 deviation using the software package Prism (Graph Pad Inc., San Diego, USA).

217

218

219 **Results and discussion**

220

221 GC–MS results

222 GC–MS analysis has here proved to be a robust and efficient technique for the rapid identification and
223 quantification of a large number of alkaloids from Amaryllidaceae plant extracts. In this study, nine
224 Brazilian species were analysed and thirty-six compounds belonging to seven skeleton-types were
225 identified (see Fig. 1; Table 1).

226 Lycorine- and homolycorine-type: an ‘ortho-para’ phenolic coupling

227 As the lycorine skeletal-type is widely distributed in the Amaryllidaceae, it was surprising to find few
228 representatives of this group in the *Hippeastrum* species and *Rodophiala bifida* surveyed. The alkaloid
229 lycorine (3) is known to be poorly soluble in both CHCl₃ and MeOH, which impedes its correct
230 quantification by GC–MS (de Andrade et al. 2012). This might explain the low relative percentage
231 observed for *H. santacatarina* (19.18 %, see Table 1), in contrast with a recent study of the same species,
232 in which it was isolated as the main compound (Giordani et al. 2011b). Overall, homolycorine-type
233 alkaloids were observed in higher variety and quantity, indicating that conversion of lycorine- to
234 homolycorine-type alkaloids is an active chemical transformation in these species.

235

236 Crinine-, haemanthamine-, tazettine-, narciclasine- and montanine-type alkaloids: a ‘para-para’ phenolic
237 coupling

238 A major mechanistic consideration in the biosynthesis of Amaryllidaceae alkaloids is ‘para-para’
239 coupling, since it gives rise to five distinct skeleton-types. The crinine-type skeleton is uncommon in the
240 genus *Hippeastrum* and the absolute configuration of its 5,10b-ethano bridge is ratified only by CD
241 spectra or X-ray crystallography (Wagner et al. 1996). As shown in Table 1 and Fig. 1, the 5,10b-
242 ethanophenanthridinealkaloids described in this study possess the haemanthamine- type skeleton as
243 previously confirmed (da Silva et al. 2008; de Andrade et al. 2011; Giordani et al. 2011a).

244 With respect to the tazettine skeleton, there are important features concerning epimerisation at C-3.

245 Duffield et al. (1965) showed that the stereochemistry of the substituent at C-3 effects marked variations
246 in the relative abundance of ions in EI-MS spectra. The b-configuration of the methoxyl group at C-3
247 facilitates a Retro-Diels–Alder (RDA) process in ring-B and loss of the neutral fragment [C₅H₈O],
248 yielding diagnostic ion peaks at 247 and m/z 231 (M–84) for tazettine (19) and deoxytazettine (17),
249 respectively. The fragment ion at m/z 70 is a small peak for both epimers (Duffield et al. 1965). As such,
250 the ion peak at m/z 70 for criwelline and 16 is much more pronounced than those observed in 17 and 19,
251 indicating that compound 16 is the 3-epideoxytazettine variant. The a-configuration of the 3-OMe
252 substituent also induces a RDA fragmentation process, but in this case with the loss of the [C₄H₈N]?
253 fragment, while the m/z 70 ion peak abundance establishes the C-3 configuration in tazettine derivatives
254 (Duffield et al. 1965).

255 In general, montanine-type alkaloids are sparsely encountered and are thus poorly represented in the
256 Amaryllidaceae. However, montanine (25) was here found as the main constituent in *H. vittatum* and *R.*
257 *bifida*, while trisphaeridine (23) was the only representative of the narciclasine-type skeleton detectable
258 as a minor compound or in trace amounts in most species (Table 1). Trisphaeridine has been considered
259 a catabolic product (Bastida et al. 2006) and this hypothesis is supported by its presence in many species
260 but hardly ever as the main alkaloid. Galanthamine-type alkaloids: a ‘para-ortho’ phenolic coupling
261 Galanthamine-type compounds were found mainly in *H. papilio* and *H. glaucescens*, with galanthamine
262 (27) being the main constituent in both cases (Table 1). Galanthamine was previously detected in *H.*
263 *papilio* (de Andrade et al. 2011), but it is here reported for the first time in *H. glaucescens*. The
264 remaining galanthamine-type representatives were detected in both species, but to a lesser extent.
265 Miscellaneous alkaloids Ismine (34) and galanthindole (35) were identified in *H. breviflorum*, *H.*
266 *morelianum*, *H. psittacinum* and *H. glaucescens*. Alkaloid 34, like 23, is also considered a catabolic
267 product arising from the haemanthamine-type skeleton (Bastida et al. 2006). Galanthindole (35) and
268 lycosinine B (36) have been considered representatives of a new skeleton containing a non-fused indole
269 ring (U’ner 2007), although the possibility that they are artifacts of homolycorine- or tazettine-type
270 derivatives cannot be overlooked.

271

272 Galanthamine quantification

273 *H. papilio* and *H. glaucescens* showed highest levels of galanthamine by GC–MS (Table 1) and the
274 availability of *H. papilio* allowed the accurate quantification of galanthamine content from dried plant
275 material. Bulbs and leaves exhibited values of 0.51 % (± 0.012) and 0.33 % (± 0.007), respectively (mg
276 GAL/100 mg DW). These values are larger than those observed for *Galanthus* and *Leucojum* species
277 used commercially by pharmaceutical companies for extraction of galanthamine (Cherkasov and
278 Tolkachev 2002; Berkov et al. 2008b, 2009). The extraction recovery was 95 % (RSD 1.73 %), 93 %
279 (RSD 2.20 %) and 91 % (RSD 0.81 %) for 50, 300 and 500 μ g of added galanthamine, respectively.
280 Intra-day repeatability ($n = 4$) expressed as RSD was determined as 1.60 for the first day and 2.21 for
281 the second, while inter-day repeatability ($n = 8$) was 2.94 with adequate values of precision (RSD ≤ 5 %).

282

283 AChE inhibitory assay for alkaloid-rich extracts

284 The results from the microplate AChE inhibition assay of plant extracts are shown in Table 2. *H. papilio*
285 and *H. glaucescens* presented the lowest IC₅₀ values as determined via the Ellman method (Section ChE
286 inhibitory activity). These are stronger activities than those observed for *Galanthus elwesii* and *G.*
287 *nivalis* (at 0.1 and 10 μ g/ml) as well as *Leucojum aestivum* (at 10 μ g/ml) (Berkov et al. 2008c). The
288 possibility of false-positive results in the AChE inhibitory activity values due to chemical inhibition
289 (Rhee et al. 2003) should not be ruled out.

290 *H. vittatum* and *R. bifida*, in which elevated levels of montanine were detected, also exhibited notable
291 AChE inhibitory effects (Table 2). Montanine (25) has previously demonstrated remarkable activity

292 against AChE obtained from rat brain, with more than 50 % inhibition at 1 mM (Pagliosa et al. 2010).
293 These results, together with psychobiological activities reported earlier for montanine (da Silva et al.
294 2006), reinforce the potential of montanine-type derivatives as therapeutic candidates for AChE
295 inhibition or other functions related to the central nervous system (da Silva et al. 2006; Pagliosa et al.
296 2010).

297

298 X-ray crystallography and AChE assay for galanthamine-derivatives

299 In agreement with previous reports (Lo'pez et al. 2002; Berkov et al. 2008c), galanthamine (27) and
300 sanguinine (28) (Fig. 4) were the most active AChE inhibitory alkaloids (IC₅₀s 0.35 and 0.06 μ M,
301 respectively). Narwedine (31) and 11b-hydroxygalanthamine (32) showed IC₅₀ values of 9.38 and 3.49
302 μ M, respectively. Some studies have been carried out to understand the binding of galanthamine and
303 galanthamine-type alkaloids at the AChE active site (Bartolucci et al. 2001; Greenblatt et al. 1999).
304 Although these have provided useful insights to the binding of the aromatic methoxyl group, the furan
305 and cyclohexene rings as well as the 3-hydroxyl substituent, the effects of the N-methyl group remain
306 largely unresolved. However, it is noteworthy that galanthamine adopted the same conformation at the
307 active site gorge as that determined by X-ray crystallographic analysis (Bartolucci et al. 2001; Carrol et
308 al. 1990).

309 The X-ray data obtained for galanthamine (27) and narwedine (31) are in agreement with previously
310 published work (Carrol et al. 1990; Hemetsberger et al. 2004). The X-ray data for sanguinine (28)¹ and
311 11b-hydroxygalanthamine (32)² are reported here for the first time. Interestingly, narwedine (31) and
312 11bhydroxygalanthamine (32) (Fig. 2) showed an axial orientation for the NMe group, opposite to that
313 seen for galanthamine. Sanguinine (28) (Fig. 3), the most potent AChE inhibitor known from the
314 Amaryllidaceae, exhibited both orientations for the NMe group with 50 % of the molecules having the
315 NMe group in the axial orientation and the other 50 % with the equatorial orientation. AChE inhibition
316 curves together with the X-ray structures of all tested galanthamine alkaloids are shown in Fig. 4.

317

318

319 **CONCLUSIONS**

320

321 Some indigenous Brazilian species are shown to produce high quantities of the AChE inhibitors
322 galanthamine and montanine. Following the approval of galanthamine by the FDA for clinical
323 management of AD, galanthamine-type alkaloids have been the most commonly studied constituents of
324 the Amaryllidaceae. Herein is reported for the first time the high levels of galanthamine detected via
325 GC–MS in *H. glaucescens*. Galanthamine levels in leaves and bulbs of *H. papilio* were higher than those
326 found in *Leucojum*, *Galanthus* and *Narcissus*, species traditionally used for commercial exploitation
327 (Berkov et al. 2009). In addition, *H. papilio* and *H. glaucescens* extracts showed the lowest IC₅₀ AChE
328 inhibition values. Since evidence from docking studies of galanthamine analogs are inconclusive, further
329 investigation is required to clarify the role of N-methyl orientation at the AChE active site gorge
330 (Bartolucci et al. 2001). Galanthamine has the N-methyl group in an equatorial disposition and showed
331 better AChE inhibitory activity than narwedine and 11b-hydroxygalanthamine, wherein the N-methyl
332 group is axially-orientated. Chlidanthine also displays an axial orientation for the N-methyl group and
333 exhibits noticeably lower AChE inhibition (IC₅₀ 24.1 μM) (Reyes-Chilpa et al. 2011). However,
334 sanguinine exhibits the best IC₅₀ inhibition values and has the N-methyl group in both axial and
335 equatorial orientations. It is known that N-methyl conformers interchange rapidly in the naturally bound
336 ligand, thereby restricting N-methyl orientation to a secondary role in new drug design. Nevertheless,
337 further protein–ligand crystallography and protein–ligand docking studies should clarify the exact role
338 of N-methyl orientation in galanthamine-type alkaloids.

339

340

341 **References**

342

343 Bartolucci C, Perola M, Christian P et al (2001) Three-dimensional structure of a complex of
344 galanthamine (Nivalin[®]) with acetylcholinesterase from *Torpedo californica*: implications for the
345 drug design of new anti-Alzheimer drugs. *Proteins* 42:182–191

346 Bastida J, Lavilla R, Viladomat F (2006) Chemical and biological aspects of *Narcissus* alkaloids.
347 In: Cordell GA (ed) *The alkaloids*, vol 63. Elsevier Inc, Amsterdam, pp 87–179

348 Berkov S, Codina C, Viladomat F et al (2008a) N-Alkylated galanthamine derivatives: potent
349 acetylcholinesterase inhibitors from *Leucojum aestivum*. *Bioorg Med Chem Lett* 18:2263–2266

350 Berkov S, Bastida J, Nikolova M et al (2008b) Analysis of galanthamine-type alkaloids by
351 capillary gas chromatography- mass spectrometry in plants. *Phytochem Anal* 19:285–293

352 Berkov S, Bastida J, Nikolova M et al (2008c) Rapid TLC/GCMS identification of
353 acetylcholinesterase inhibitors in alkaloids extracts. *Phytochem Anal* 19:411–419

354 Berkov S, Georgieva L, Kondakova V et al (2009) Plant source of galanthamine: phytochemical
355 and biotechnological aspects. *Biotechnol Biotechnol Equip* 23:1170–1176

356 Berkov S, Bastida J, Viladomat F et al (2011) Development and validation of a GC-MS method for
357 a rapid determination of galanthamine in *Leucojum aestivum* and *Narcissus* ssp.: A metabolomic
358 approach. *Talanta* 83:1455–1465

359 Carrol P, Furst GT, Han SY et al (1990) Spectroscopic studies of galanthamine and galanthamine
360 methiodide. *Bull Soc Chim Fr* 127:769–780

361 Castilhos TS, Giordani RB, Henriques AT et al (2007) Avaliação in vitro das atividades
362 antiinflamatória, antioxidante e antimicrobiana do alcaloide montanina. *Rev Bras Farmacogn*
363 17:209–214

364 Cherkasov OA, Tolkachev ON (2002) *Narcissus* and other Amaryllidaceae as sources of galanthamine.
365 In: Hanks G (ed) *Medicinal and aromatic plants—industrial profiles: Narcissus and Daffodil, the*
366 *genus Narcissus*. Taylor and Francis, London and New York, pp 242–255

367 C, itog˘lu G, Tanker M, Gu˘mu˘s,el B (1998) Antiinflammatory effects of lycorine and haemanthidine.
368 *Phytother Res* 12:205–206

369 da Silva AFS (2005) *Hippeastrum vittatum* (L'Her) Herbert e *Hippeastrum striatum* (Lam.) Moore:
370 Análise química e avaliação biológica dos alcaloides isolados. Dissertation, Universidade
371 Federal do Rio Grande do Sul

372 da Silva AFS, de Andrade JP, Bevilaqua LR et al (2006) Anxiolytic-, antidepressant- and
373 anticonvulsivant-like effects of the alkaloid montanine isolated from *Hippeastrum vittatum*.
374 *Pharmacol. Biochem Behav* 85:148–154

375 da Silva AFS, de Andrade JP, Machado KRB et al (2008) Screening for cytotoxic activity of
376 extracts and isolated alkaloids from bulbs of *Hippeastrum vittatum*. *Phytomedicine* 15:882–885

377 de Andrade JP, Berkov S, Viladomat F et al (2011) Alkaloids from *Hippeastrum papilio*.
378 *Molecules* 16:7097–7104

379 de Andrade JP, Pigni NB, Torras-Claveria L et al (2012) Bioactive alkaloids from *Narcissus*
380 *broussonetii*: mass spectral studies. *J Pharm Biomed Anal* 70:13–25

381 Duffield AM, Aplin RT, Budzikiewicz H et al (1965) Mass spectrometry in structural and
382 stereochemical problems. LXXXII. A study of the fragmentation of some Amaryllidaceae
383 alkaloids. *J Am Chem Soc* 87:4902–4912

384 Giordani RB, Vieira PB, Weizenmann M et al (2010) Candimine-induced cell death of the
385 amitochondriate parasite *Trychomonas vaginalis*. *J Nat Prod* 73:2019–2023

386 Giordani RB, de Andrade JP, Verli H et al (2011a) Alkaloids from *Hippeastrum morelianum* Lem.
387 (Amaryllidaceae). *Magn Reson Chem* 49:668–672

388 Giordani RB, Vieira PB, Weizenmann M et al (2011b) Lycorine induces cell death in the
389 amitochondriate parasite, *Trichomonas vaginalis*, via an alternative non-apoptotic death pathway.
390 *Phytochemistry* 72:645–650

391 Greenblatt HM, Kryger G, Lewis T et al (1999) Structure of acetylcholinesterase complexed
392 with (-)-galanthamine at 2.3 Å resolution. *FEBS Lett* 463:321–326

393 Hemetsberger M, Treu M, Jordis U et al (2004) 1-methylgalanthamine derivatives. *Monatsh Chem*
394 135:1275–1287

395 International Tables of X-Ray Crystallography (1974) Kynoch Press. Birmingham

396 Kreh M, Matusch R, Witte L (1995) Capillary gas chromatography-mass spectrometry of
397 Amaryllidaceae alkaloids. *Phytochemistry* 38:773–776

398 Lo'pez S, Bastida J, Viladomat F et al (2002) Acetylcholinesterase inhibitory activity of some
399 Amaryllidaceae alkaloids and *Narcissus* extracts. *Life Sci* 71:2521–2529 Machocho AK, Bastida
400 J, Codina C et al (2004) Augustamine type alkaloids from *Crinum kirkii*. *Phytochemistry*
401 65:3143–3149

402 Maelicke A, Samochocki M, Jostock R et al (2001) Allosteric sensitization of nicotinic receptors by
403 galantamine, a new treatment strategy for Alzheimer's disease. *Biol Psychiatry* 49:279–288

404 McNulty J, Nair JJ, Codina C et al (2007) Selective apoptosis-inducing activity of crinum-type
405 Amaryllidaceae alkaloids. *Phytochemistry* 68:1068–1074

406 McNulty J, Nair JJ, Singh M et al (2009) Selective cytochrome P450 3A4 inhibitory activity of
407 Amaryllidaceae alkaloids. *Bioorg Med Chem Lett* 19:3233–3237

408 Pagliosa LB, Monteiro SC, Silva KB et al (2010) Effect of isoquinoline alkaloids from two
409 *Hippeastrum* species on in vitro acetylcholinesterase activity. *Phytomedicine* 17:698–701

410 Reyes-Chilpa R, Berkov S, Hernández-Ortega S et al (2011) Acetylcholinesterase inhibiting
411 alkaloids from *Zephyranthes concolor*. *Molecules* 16:9520–9533

412 Rhee IK, van Rijn RM, Verpoorte R (2003) Qualitative determination of false-positive effects in
413 the acetylcholinesterase assays using thin layer chromatography. *Phytochem Anal* 14:127–131

- 414 Sebben C (2005) Investigac,ao qu' mica e biolo'gica em *Hippeastrum breviflorum* Herb.
415 (Amaryllidaceae). Dissertation, Universidade Federal do Rio Grande do Sul
- 416 Sheldrick GM (2008) A program for automatic solution of crystal structure refinement. *Acta*
417 *Crystallogr A* 64:112–221
- 418 U'nver N (2007) New skeletons and new concepts in Amaryllidaceae alkaloids. *Phytochem Rev*
419 6:125–135
- 420 Vrijssen R, Berghe DAV, Vlietinck AJ et al (1986) Lycorine: an eukaryotic terminator inhibitor? *J*
421 *Biol Chem* 261:505–507
- 422 Wagner J, Pham HL, Do'pke W (1996) Alkaloids from *Hippeastrum equestre* Herb. -5. Circular
423 dichroism studies. *Tetrahedron* 52:6591–6600
- 424 Wagner C, Sefkow M, Kopka J (2003) Construction and application of a mass spectral and
425 retention time index database generated from plant GC/EI-TOF-MS metabolite profiles.
426 *Phytochemistry* 62:887–900
- 427 Zupko' I, Re'thy B, Hohmann J et al (2009) Antitumor activity of alkaloids derived from
428 Amaryllidaceae species. *In Vivo* 23:41–48
- 429

430 **Legends to figures**

431

432 **Fig. 1** Alkaloids found in the Brazilian species

433

434 **Fig. 2** ORTEP projection of 11b-hydroxygalanthamine (32)

435

436 **Fig. 3** Top, a view of the molecular structure of compound 3. Bottom, the labeled core of the cubane.

437 Bonds depicted in orange correspond to the short Cu–O distances inside the {Cu₄O₄} cage and the

438 dashed red bonds show the H-bonds involving the coordinated water molecule

439

440 **Scheme 3** ORTEP projection of sanguinine (28)

441

442 **Fig. 4** Acetylcholinesterase inhibition curve and X-ray structures of sanguinine, galanthamine, 11b-

443 hydroxygalanthamine and narwedine showing the N-methyl orientation

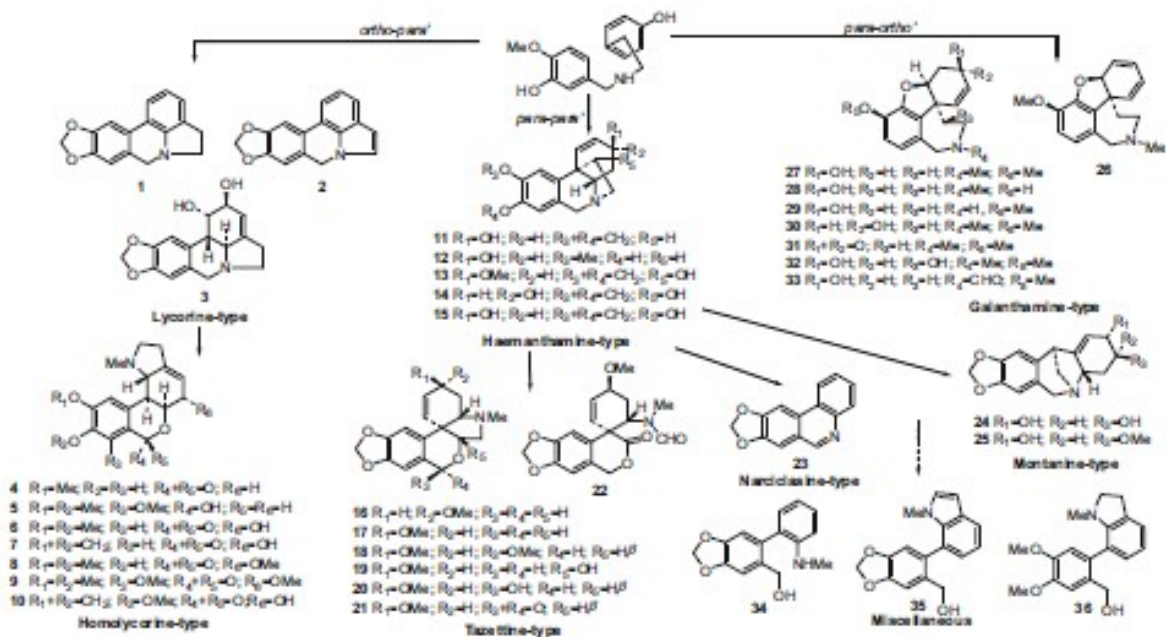
444

445

446

447
448
449

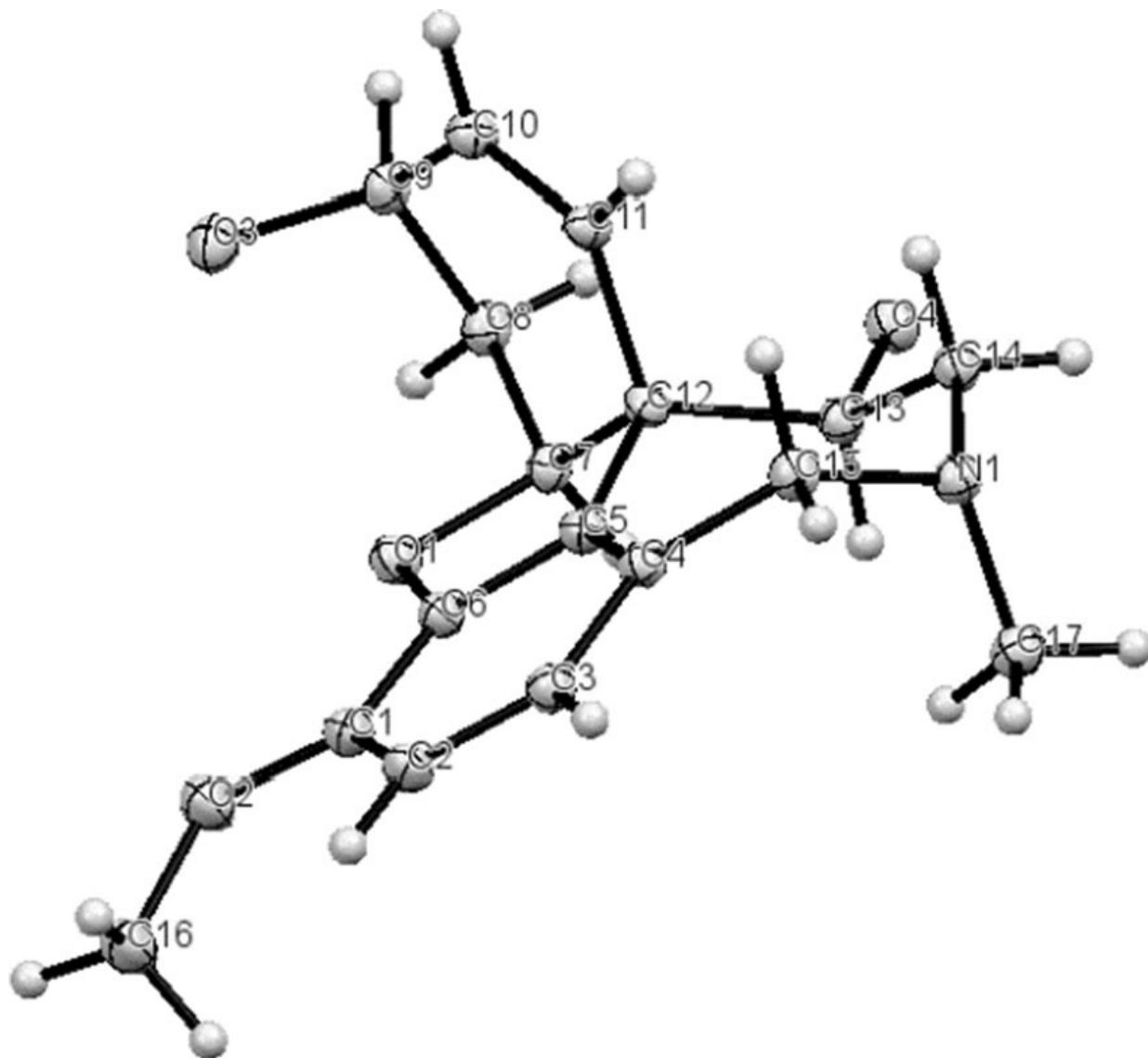
FIGURE 1



450
451

452
453
454

FIGURE 2

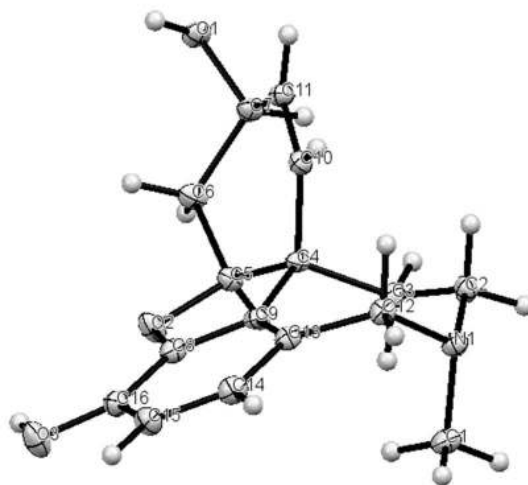
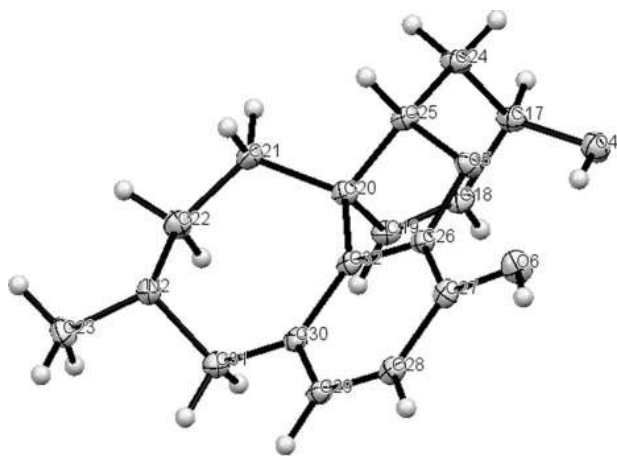


455
456
457

458

FIGURE 3

459



460

461

FIGURE 4

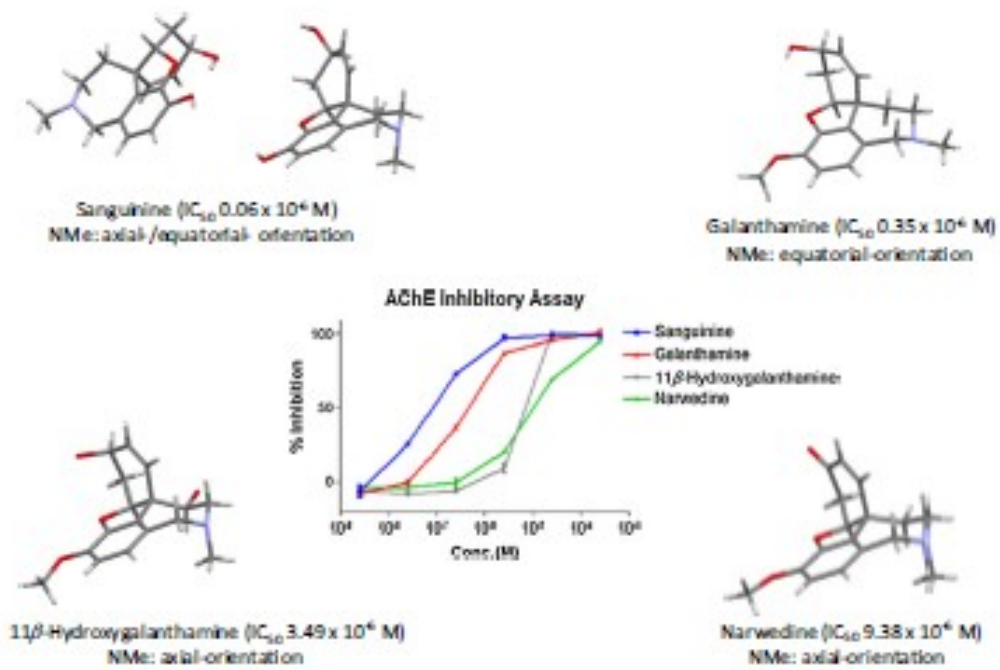


Table 1 Alkaloids found in several Brazilian species. Values are expressed as a relative percentage of TIC

Compound	RI	M ⁺	Rel. int. (%)	<i>H. virianum</i>		<i>H. breviflorum</i>		<i>H. macranthum</i>		<i>H. papilio</i>	
				Bulbs	Leaves	Bulbs	Leaves	Bulbs	Leaves	Bulbs	Leaves
Anhydrolycorine (1)	2501	251 (43)	250 (100), 192 (13), 191 (11), 165 (4), 164 (3), 139 (2), 124 (7)	-	-	-	-	-	-	-	-
11,12-Dihydroanhydrolycorine (2)	2606	249 (60)	248 (100), 191 (10), 190 (24), 189 (7), 163 (7), 95 (17)	-	1.17	-	-	-	-	-	-
Lycorine (3)	2746	287 (31)	286 (19), 268 (24), 250 (15), 227 (79), 226 (100), 211 (7), 147 (15)	tr	-	-	-	-	-	-	-
8-O-Demethylhomolycorine (4)	2841	301 (-)	192 (0.5), 164 (2), 110 (8), 109 (100), 108 (23), 94 (3), 82 (3)	-	-	-	-	-	-	-	-
Nerine (5)	2476	347 (-)	330 (7), 329 (3), 236 (1), 221 (9), 191 (2), 109 (100), 94 (2)	-	-	1.86	-	-	-	-	-
2α-Hydroxyhomolycorine (6)	2970	331 (-)	178 (3), 126 (8), 125 (100), 124 (7), 96 (31), 94 (4)	-	-	-	tr	-	-	-	-
Hippeastrine (7)	2917	315 (-)	190 (1), 162 (4), 134 (2), 125 (100), 96 (40), 82 (3)	-	-	-	-	-	-	-	-
2α-Methoxyhomolycorine (8)	2870	345 (-)	178 (5), 140 (11), 139 (100), 124 (67), 94 (7), 77 (5)	-	-	-	-	-	-	-	-
2α,7-Dimethoxyhomolycorine (9)	2962	375 (-)	221 (2), 140 (9), 139 (100), 125 (6), 124 (55), 94 (4)	-	-	-	-	-	-	-	-
Cardimine (10)	3070	345 (-)	192 (1), 177 (2), 163 (1), 147 (1), 125 (100), 96 (30), 82 (2)	-	-	-	-	-	-	-	-
Viratine (11)	2472	271 (100)	272 (20), 252 (35), 199 (70), 187 (61), 173 (22), 115 (28)	1.23	-	-	-	-	-	-	tr
8-O-Demethylmaritidine (12)	2510	273 (100)	274 (17), 230 (24), 201 (83), 189 (52), 175 (20), 115 (18)	1.62	-	-	-	-	-	tr	-
Hamantamine (13)	2641	301 (13)	272 (100), 240 (16), 211 (13), 199 (7), 181 (21), 153 (8)	-	-	-	-	-	-	16.16	21.60
Hamayne (14)	2699	287 (5)	259 (18), 258 (100), 214 (10), 186 (14), 181 (14), 115 (13)	-	-	-	-	-	-	-	-
11-Hydroxyviratine (15)	2728	287 (6)	259 (18), 258 (100), 242 (10), 211 (15), 181 (20), 128 (13)	-	-	-	-	-	-	-	-
3-Epideoxyviratine (16)	2241	315 (21)	300 (41), 232 (14), 231 (100), 185 (12), 115 (15), 70 (65)	-	-	3.12	-	-	-	-	-
Doxyviratine (17)	2486	315 (21)	300 (15), 260 (5), 231 (100), 227 (10), 211 (15), 197 (10), 115 (9)	-	-	4.10	-	-	-	-	-

Table 1 continued

Compound	RI	M ⁺	Rel. int. (%)	<i>H. striatum</i> Bulbs	<i>H. vitatum</i> Bulbs	<i>H. breviflorum</i> Bulbs	<i>H. moreletianum</i> Bulbs	<i>H. papilio</i> Bulbs	<i>H. papilio</i> Leaves
6-Methoxyprocaine (18)	2610	345 (26)	330 (21), 262 (21), 261 (100), 239 (40), 228 (30), 201 (28)	-	-	tr	-	-	-
Tuacetine (19)/Procaine (20)*	2653	331 (31)	316 (15), 298 (23), 247 (100), 230 (12), 201 (15), 181 (11), 152 (7)	-	-	26.50	58.83	-	-
3-Epinacrine (21)	2811	329 (27)	314 (23), 245 (100), 225 (14), 201 (83), 139 (16), 70 (18)	-	-	0.63	3.18	-	-
Tacetamide (22)	2914	313 (30)	260 (100), 229 (20), 201 (49), 171 (12), 143 (9), 115 (26)	-	-	-	tr	-	-
Triphacetidine (23)	2282	223 (100)	222 (38), 167 (8), 165 (9), 164 (14), 138 (20), 137 (9), 111 (13)	tr	-	0.75	1.5	-	-
Piacrine (24)	2718	287 (100)	270 (22), 243 (22), 223 (25), 199 (29), 185 (34), 115 (18)	-	tr	-	-	-	-
Moxazine (25)	2611	301 (100)	270 (90), 257 (39), 252 (26), 223 (33), 185 (37), 115 (30)	86.62	-	-	-	-	-
Anhydrogalanthamine (26)	1766	269 (100)	268 (38), 211 (43), 195 (22), 193 (31), 165 (61), 115 (26)	-	-	-	-	1.32	-
Galanthamine (27)	2395	287 (83)	288 (14), 286 (100), 270 (13), 244 (26), 216 (37), 174 (34)	-	-	-	tr	63.24	58.97
Sanguinine (28)	2422	273 (100)	272 (79), 256 (18), 216 (18), 202 (37), 160 (44), 115 (25)	-	-	-	-	-	tr
N-Demethylgalanthamine (29)	2442	273 (98)	272 (100), 230 (44), 202 (34), 201 (12), 174 (13)	-	-	-	-	-	-
3-Epialantamine (30)	2443	287 (77)	286 (100), 270 (15), 244 (16), 216 (70), 211 (14), 174 (26)	-	-	-	-	-	-
Narwedine (31)	2483	285 (95)	284 (100), 242 (30), 228 (25), 216 (40), 199 (35), 174 (40)	-	-	-	-	1.62	2.85
11β-Hydroxyalantamine (32)	2597	303 (24)	231 (21), 230 (100), 213 (27), 181 (13), 174 (13), 115 (15)	-	-	-	-	3.80	9.65
N-Formylgalanthamine (33)	2816	301 (100)	230 (9), 225 (16), 211 (18), 165 (9), 128 (10), 115 (13)	-	-	-	-	-	-
Ismitine (34)	2280	257 (35)	238 (100), 211 (6), 196 (8), 168 (6), 154 (3), 106 (4), 77 (3)	-	-	1.41	0.75	-	-
Galanthidole (35)	2487	281 (100)	280 (7), 264 (13), 263 (17), 262 (20), 252 (15), 191 (14)	-	-	1.70	1.49	-	-
Lycotinine B (36)	2520	297 (100)	298 (19), 269 (72), 268 (56), 254 (32), 237 (19), 222 (16)	-	-	5.12	-	-	-

Table 1 continued

Compound	RI	M ⁺	Rel. int. (%)	<i>H. peiracium</i> Bulbs	<i>H. peiracium</i> Leaves	<i>H. semicarpina</i> Leaves	<i>H. glaucescens</i> Bulbs	<i>H. glaucescens</i> Leaves	<i>R. bifida</i> Bulbs
Anhydrolycorine (1)	2501	251 (43)	250 (100), 192 (13), 191 (11), 165 (4), 164 (3), 139 (2), 124 (7)	-	-	tr	-	-	-
11,12-Dehydroanhydrolycorine (2)	2606	249 (60)	248 (100), 191 (10), 190 (24), 189 (7), 163 (7), 95 (17)	-	-	14.64	-	-	-
Lycorine (3)	2746	287 (31)	286 (19), 268 (24), 250 (15), 227 (79), 226 (100), 211 (7), 147 (15)	-	-	19.18	-	-	-
8-O-Demethylhomolycorine (4)	2841	301 (-)	192 (0.5), 164 (2), 110 (8), 109 (100), 108 (23), 94 (3), 82 (3)	-	0.61	-	-	-	-
Nerine (5)	2476	347 (-)	330 (7), 329 (5), 236 (1), 221 (9), 191 (2), 109 (100), 94 (2)	-	-	-	-	-	-
2 α -Hydroxyhomolycorine (6)	2970	331 (-)	178 (3), 126 (6), 125 (100), 124 (7), 96 (31), 94 (4)	-	-	-	-	-	-
Hippeastrine (7)	2917	315 (-)	190 (1), 162 (4), 134 (2), 125 (100), 96 (40), 82 (3)	8.82	23.90	-	-	tr	-
2 α -Methoxyhomolycorine (8)	2870	345 (-)	178 (5), 140 (11), 139 (100), 124 (67), 94 (7), 77 (5)	-	-	-	-	-	-
2 α -7-Dimethoxyhomolycorine (9)	2962	375(-)	221(2), 140(9), 139(100), 125(6), 124(5), 94(4)	-	-	-	-	-	-
Candimine (10)	3070	345 (-)	192 (1), 177 (2), 163 (1), 147 (1), 125 (100), 96 (30), 82 (2)	-	-	-	-	-	-
Veratrine (11)	2472	271 (100)	272 (20), 252 (35), 199 (70), 187 (61), 173 (22), 115 (28)	-	-	tr	-	-	tr
8-O-Demethylmaridine (12)	2510	273 (100)	274 (17), 230 (24), 201 (83), 189 (52), 175 (20), 115 (18)	-	-	-	-	-	-
Hacmaridine (13)	2641	301 (13)	272 (100), 240 (16), 211 (13), 199 (7), 181 (21), 153 (8)	-	-	3.61	-	-	-
Hamayne (14)	2699	287 (5)	259 (18), 258 (100), 214 (10), 186 (14), 181 (14), 115 (13)	-	-	-	-	-	-
11-Hydroxyveratrine (15)	2728	287(6)	259(18), 258(100), 242(10), 211(15), 181(20), 128(13)	-	-	8.51	-	-	-
3-Epihydroxyveratrine (16)	2241	315 (21)	300 (41), 232 (14), 231 (100), 185 (12), 115 (15), 70 (65)	-	-	-	1.26	-	-
Deoxyveratrine (17)	2486	315 (21)	300 (15), 260 (5), 231 (100), 227 (10), 211 (15), 197 (10), 115 (9)	tr	0.82	tr	0.30	tr	tr

Table 1 continued

Compound	RI	M ⁺	Rel. int. (%)	<i>H. psittacinum</i> Bulbs	<i>H. psittacinum</i> Leaves	<i>H. santatarina</i> Leaves	<i>H. glaucocens</i> Bulbs	<i>H. glaucocens</i> Leaves	<i>R. bifida</i> Bulbs
6-Methoxypretazetamine (18)	2610	345 (26)	330 (21), 262 (21), 228 (30), 201(28)	261 (100), 239 (40),	-	-	-	-	-
Tazetamine (19)/Pretazetamine (20)*	2653	331 (31)	316 (15), 298 (23), 201 (15), 181 (11), 152 (7)	247 (100), 230 (12),	14.83	tr	7.62	14.89	tr
3-Epimacronine (21)	2811	329 (27)	314 (23), 245 (100), 139 (16), 70 (18)	225 (14), 201 (83),	7.31	tr	0.91	3.64	tr
Taxetamide (22)	2914	313 (30)	260 (100), 229 (20), 143 (9), 115 (20)	201 (49), 171 (12),	1.27	-	-	-	-
Triphacetidine (23)	2282	223 (100)	222 (88), 167 (6), 20, 137 (9), 111 (13)	164 (14), 138 (20), 111 (13)	tr	19.34	0.63	tr	-
Pancracine (24)	2718	287 (100)	270 (22), 243 (22), 185 (34), 115 (18)	223 (25), 199 (29),	-	-	-	-	-
Montanine (25)	2611	301 (100)	270 (90), 257 (39), 183 (37), 115 (30)	252 (26), 223 (33),	-	-	-	-	91.94
Anhydrogalanthamine (26)	1766	269 (100)	268 (38), 211 (43), 165 (61), 115 (26)	195 (22), 193 (31),	-	-	16.38	tr	-
Galanthamine (27)	2395	287 (83)	288 (14), 286 (100), 216 (37), 174 (34)	270 (13), 244 (26),	tr	tr	5.30	65.15	-
Sanguinine (28)	2422	273 (100)	272 (79), 256 (18), 160 (44), 115 (25)	216 (18), 202 (37),	-	-	1.38	tr	-
4-Deacetyl galanthamine (29)	2442	273 (98)	272 (100), 230 (44), 174 (13)	202 (34), 201 (12),	-	-	tr	-	-
3-Epigalanthamine (30)	2443	287 (77)	286 (100), 270 (15), 211 (14), 174 (26)	244 (16), 216 (70),	-	-	2.23	-	-
Narwedine (31)	2483	285 (95)	284 (100), 242 (30), 199 (35), 174 (40)	228 (25), 216 (40),	-	-	5.51	2.42	-
11β-Hydroxy galanthamine (32)	2597	303 (24)	231 (21), 230 (100), 174 (13), 115 (15)	213 (27), 181 (13),	-	-	-	-	-
4-Formylgalanthamine (33)	2816	301 (100)	230 (9), 225 (16), 110, 115 (13)	211 (18), 165 (9), 128 (10), 115 (13)	-	-	-	tr	-
Isomine (34)	2280	257 (35)	238 (100), 211 (6), 106 (8), 77 (3)	196 (8), 168 (6), 154 (3), 106 (4), 77 (3)	10.46	-	-	2.10	-
Galanthindole (35)	2487	281 (100)	280 (7), 264 (13), 15, 191 (14)	263 (17), 262 (20), 252 (15), 191 (14)	12.73	-	-	-	5.41
Lycocaine B (36)	2520	297 (100)	298 (19), 269 (72), 237 (19), 222 (16)	268 (56), 254 (32),	-	-	-	-	-

* Pretazetamine (20) is quantified as tazetamine (19) (de Andrade et al. 2012); Values <0.20 were assumed as "traces" (tr)

486 **Table 2** AChE inhibitory activity of the alkaloid extracts
 487

Plant species	IC ₅₀ (µg/ml)	AChE inhibition %	
		10 µg/ml	0.1 µg/ml
<i>Hippeastrum striatum</i> bulbs	nd	-	-
<i>Hippeastrum vitatum</i> bulbs	4.67	31.0	2.0
<i>Hippeastrum breviflorum</i> bulbs	nd	-	-
<i>Hippeastrum morelianum</i> bulbs	nd	-	-
<i>Hippeastrum papilio</i> bulbs	0.45	93.0	23.0
<i>Hippeastrum papilio</i> leaves	0.41	96.0	24.0
<i>Hippeastrum psittacinum</i> bulbs	nd	-	-
<i>Hippeastrum psittacinum</i> leaves	nd	-	-
<i>Hippeastrum santacatarina</i> bulbs	nd	-	-
<i>Hippeastrum glaucescens</i> bulbs	0.33	93.0	26.0
<i>Hippeastrum glaucescens</i> leaves	0.49	94.0	20.0
<i>Hippeastrum aulicum</i> leaves	nd	-	-
<i>Rhodophiala bifida</i> bulbs	8.45	28.0	3.0

488